Adapting a compact Mott spin polarimeter to a large commercial electron energy analyzer for spin-polarized electron spectroscopy

Di-Jing Huang, Jae-Yong Lee, Jih-Shih Suen, G. A. Mulhollan, A. B. Andrews, and J. L. Erskine
Department of Physics, University of Texas at Austin, Austin, Texas 78712-1081

(Received 6 July 1993; accepted for publication 16 December 1993)

A modified Rice University-type compact Mott spin polarimeter operating at 20 kV is adapted to a large commerical hemispherical electron energy analyzer. Normal energy analyzer functions are preserved via a retractable channeltron in the polarimeter acceleration column. In the spin-detection mode, the polarimeter permits analysis of two orthogonal transverse spin-polarization components. Electron trajectory analysis is used to optimize polarimeter lens column voltages in both normal and spin-detection modes. Performance levels are established by experiments and significantly improved spin-detection efficiency is shown to be accessible by changes in the polarimeter collection solid angle.

I. INTRODUCTION

Electron-spin-polarization analysis has been used to great advantage in a variety of fields.[1] Particularly fruitful have been investigations of surface and ultrathin film magnetism with this technique.[2] The addition of electron spin detection extends Auger electron spectroscopy (AES), electron spectroscopy for chemical analysis (ESCA), and angle-resolved photoemission by permitting detailed experimental studies of the rich variety of magnetic and other spin-dependent phenomena associated with magnetic surfaces, thin films, and multilayers.

While a variety of spin-polarization detection methods have been developed, the Mott polarimeter remains the most widely used electron-spin-polarization analyzer. This type of spin-polarization measurement is based on Mott scattering.[3] When high-energy (10–300 keV) spin-polarized electrons are scattered at large angles from a nucleus of atomic number Z, the spin-orbit interaction causes a left–right spatial scattering asymmetry defined as

$$A=\frac{I_L-I_R}{I_L+I_R}, \tag{1}$$

where I_L and I_R are the scattered intensities into equivalent left-hand and right-hand solid angles, respectively. The spin-orbit interaction strength for bound electrons is proportional to the fourth power of Z, and Mott scattering also reflects a strong Z dependence. Thus, high-Z materials are favored as the scattering medium. The spin-polarization component P measured normal to the scattering plane is proportional to the scattering asymmetry, i.e.,

$$A=SP, \tag{2}$$

where S is an energy- and angle-dependent quantity called the Sherman function.

Two important parameters are generally used to characterize the performance of Mott polarimeters. They are the sensitivity, defined as I/I_0, and the efficiency, defined as

$$\epsilon=S^2(I/I_0), \tag{3}$$

where I_0 is the current entering the polarimeter, and I is the total current ($I=I_L+I_R$) detected after scattering. The parameter ϵ is often referred to as the figure of merit for the spin detector since it is proportional to the inverse square of the statistical error in an electron counting measurement that determines the polarization P of an incident beam. Typical values for the sensitivity and efficiency of Mott polarimeters are $I/I_0\sim10^{-4}$–10^{-2} and $\epsilon\sim10^{-5}$–10^{-4}. It is clear from these parameters that a spectrometer intended for use in both spin-polarized and spin-integrated detection experiments should employ a separate detection scheme when electron-spin detection is not required in order to avoid the enormous loss of efficiency associated with the large-angle scattering. This requirement represents one important criteria for our spin-polarimeter/detection system.

II. SELECTION OF SPIN POLARIMETER: ELECTRON OPTICAL ACCEPTANCE

We chose to adapt a Rice University-type Mott spin polarimeter to a large commerical electron energy analyzer (VSW HA-150) because this combination offers versatile performance for a broad range of applications. Our intended applications included use at a synchrotron radiation beamline (spin-polarized valence band and core-level experiments) as well as general purpose applications including AES and ESCA utilizing typical laboratory sources such as electron guns and fixed anode x-ray sources. The large mean radius ($r_0=150$ mm) is necessary to improve sensitivity in applications using low-brightness sources, such as a commerical laboratory x-ray source. The HA-150 lens column, shown schematically in Fig. 1, incorporates a lens near the target (permitting a large electron acceptance angle) and a pair of apertures in a constant field region between tandem lens stacks that can be used to electronically vary the analyzer angular acceptance. By suitable choice of lens column voltages, the collection angle can be varied from approximately 1°, which we find useful for angle-resolved photoemission and electron forward scattering experiments, to about 22°, which yields the high collection efficiency required for high-resolution ESCA as

 0034-6748/93/64(12)/3474/6/$6.00

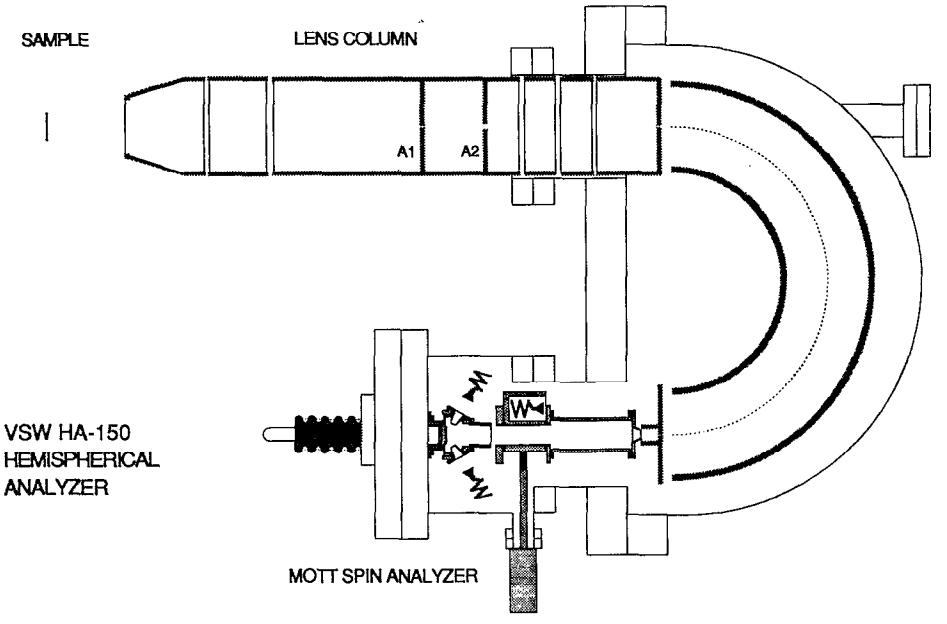

FIG. 1. Cross-sectional view of a VSW HA-150 electron energy analyzer showing a micro-Mott spin polarimeter adapted to the exit slit flange.

well as spin-detection experiments of all types including spin-polarized AES and spin-polarized secondary electron analysis.

Several electron-spin-polarization detector designs were considered. Polarimeters based on low-energy (150-eV) diffuse scattering from an evaporated (polycrystalline) gold surface have been developed.[4,5] These polarimeters offer relatively high efficiency ($\epsilon \sim 2\times 10^{-4}$), compact size, and the absence of problems associated with high voltage. A second type of low-voltage polarimeter is based on spin-dependent elastic scattering from a single-crystal tungsten surface.[6,7] This low-energy-electron-diffraction (LEED)-type spin detector achieves efficiency comparable to the diffuse scattering polarimeter. A third type of spin polarimeter, which can be considered different from the conventional 100-kV Mott detector,[8] is the compact Rice University-type Mott polarimeter,[9,10] which operates at 20–40 kV.

Several factors were considered in deciding which spin polarimeter would best meet our requirements. The low-voltage (LEED-type and diffuse-scattering) polarimeters are compact, efficient, and avoid high-voltage problems. However, because of the low scattering energy where electron mean free paths in metals are short, and near-surface scattering dominates, their performance is strongly affected by surface conditions of the scattering medium. Scattering target surfaces must be maintained in a UHV environment, cleaned periodically, or renewed frequently by evaporating a new layer. In addition, periodic calibration and performance checks are required due to the high sensitivity of low voltage polarimeters to surface conditions. The higher-voltage micro-Mott (here defined as compact Mott-type polarimeters operating at $\sim$20 kV) and conventional Mott polarimeters are insensitive to the scattering surface condition and offer more stable calibrations and performance levels. On the other hand, the 20-kV micro-Mott polarimeter designs have not yet achieved efficiencies equivalent to those reported for low-energy spin detectors. However, none of these factors were judged as decisive in choosing between the various polarimeter options.

Several factors were considered very important in our decision to adapt a 20-kV micro-Mott design. The two most important considerations are related and are associated with the sensitivity of polarimeter asymmetry to input beam conditions and the polarimeter electron-optical acceptance phase space, defined as

$$\Phi = A\Omega E, \tag{4}$$

where A is the beam cross section, Ω is the angular spread, and E is the beam energy, all defined at a plane intersecting the beam. The parameter Φ has an important property: In a paraxial electron-optical system in which electron current is conserved, the Helmholtz–Lagrange law states that Φ is conserved.

All spin polarimeters depend on scattering intensity right–left asymmetry to measure spin polarization, and are therefore subject to instrumental asymmetries resulting from variations in incident beam conditions independent of the beam's spin polarization. For example, the LEED-type polarimeter requires a well-collimated beam with narrow angular spread because the asymmetry is detected in Bragg peaks that are sensitive to both the energy and angle of incident electrons. The instrumental asymmetries of low-energy diffuse-scattering detectors depend on geometrical factors that determine detection solid angles after scattering and on the stability of the beam position and profile at the scattering target. In general, low-energy spin polarimeters require spatially stable well-collimated beams to perform well, and because the scattering occurs at relatively low energy, they have a maximum acceptance phase space limited to approximately 10^2 mm^2 sr eV.[11]

Polarimeters operating at high voltages (20 kV) offer several important advantages in terms of acceptance phase space and insensitivity to input beam conditions.[12] In our application, the maximum accessible electron-optical phase space is determined by the electron energy analyzer. The energy resolution ΔE of a hemispherical analyzer operated at optimum étendue[13] is given by[14]

$$\frac{\Delta E}{E_0}=\frac{w}{2r_0}+\alpha^2, \tag{5}$$

where w is the slit width, r_0 is the analyzer mean radius, α is the beam angle at the slits, and E_0 is the pass energy. Assuming identical rectangular slits having dimensions $w=6$ mm and $h=12$ mm, and equal contributions to ΔE from the w (slit width) and α^2 terms in Eq. (5), the electron optical phase space defined by Eq. (4) for a 150-mm mean radius analyzer is approximately $\Phi_m=4.5E_0$ mm^2 sr eV. For moderate resolving power (1%), E_0 is typically chosen to be 50 eV for analyzing Auger lines, and the maximum phase space is $\Phi_m=225$ mm^2 sr eV, a value that could not be accommodated by a low-energy spin detector. When analyzing the spin polarization of secondary electrons, the energy resolution is usually of little importance, and the analyzer is operated at maximum transmission.

We have gained useful practical experience using a low-energy diffuse scattering spin polarimeter in an application that presents more favorable experimental parameters for a low-energy spin polarimeter than our present application. A low-energy diffuse scattering spin polarimeter has been adapted to a 50-mm mean radius hemispherical electron energy analyzer for spin-polarized angle-resolved photoemission spectroscopy. The analyzer has a nominal (fixed) angular resolution of $\pm 1.5°$, and is used at beamline U5 of the National Synchrotron Light Source. The undulator source and 6-m monochromator define a small (<1 mm^2) illuminated region on the magnetic surfaces that are studied. An estimate of the analyzer acceptance phase space for this application yields $\Phi_m=0.5E_0$ mm^2 sr eV (analyzer luminosity scales as r_0^2). In typical applications, $\Delta E/E_0\sim 0.01$ and $E_0\sim 30$ eV so the analyzer electron-optical phase space admitted into the low-energy spin detector is approximately 15 mm sr eV, clearly small compared to the calculated maximum value ($\sim 10^2$) for this type of polarimeter. However, minor spatial instabilities in the storage ring electron beam, which are manifested as small variations in the monochromator focus position on the sample, were found to produce nonstatistical errors in detected spin polarization. There are limited options for dealing with these types of errors: (i) stabilize the beam, (ii) increase detection efficiency so that shorter integration times lead to smaller nonstatistical errors, (iii) compensate for the asymmetry in the spin detector,[15] or (iv) use a spin detector with inherently less sensitivity to input beam conditions.

The sensitivity of the low-energy diffuse scattering spin detector to spatial instabilities associated with the source have been significantly reduced by an improved design[4] that functions quite well at the beamline facility. These detectors also appear to function extremely well when a high-brightness electron source is used, as in typical scanning electron microscope with polarization analysis (SEMPA) applications,[5] where a high spatial resolution electron beam creates (low-energy) polarized secondary electrons from a very small source region. However, our applications include larger source areas and higher electron kinetic energies. These requirements suggest that a high-voltage Mott-type spin polarimeter would be a more appropriate choice. In addition, the extremely high acceleration ratio associated with a high-voltage Mott detector produces a small and very stable scattering region at the Au foil target. High-voltage Mott polarimeters are quite insensitive to incident beam instabilities, especially in a case where the source region, in this case, the exit slit of the electron energy analyzer, is mechanically referenced to the Mott detector acceleration column.

III. DESCRIPTION OF POLARIMETER

Figure 2 presents a cross-sectional view of our modified Rice University-type micro-Mott polarimeter mounted to the exit slit port of an HA-150 electron energy analyzer. Several minor modifications were made in the original design to meet specific requirements for our application. Our polarimeter incorporates four channeltrons that detect asymmetric scattering in two orthogonal planes, permitting both in-plane polarization components to be determined simultaneously. The polarimeter acceleration lens column was lengthened to simplify mechanical design of the detector housing. The longer acceleration column also permitted convenient mounting of a fifth channeltron detector in a block having two parallel holes bored in it. One hole serves as a tube lens in the acceleration column when spin detection is required. The second hole serves as a housing for the fifth channeltron used for detecting electrons in experiments not requiring spin analysis. A linear motion feedthrough permits selecting either the channeltron or lens tube position of the block in the lens column.

Mechanical details of the sliding channeltron housing are shown in Fig. 2. The sliding lens block is guided by grooves milled in the block at both ends. Ball bearings, mounted in the lens column, fit in the grooves, and serve to center as well as guide the block. The lens block is electrically isolated from the (grounded) mechanical feedthrough by a ceramic coupling. The sliding block assembly is accommodated by the vacuum vessel originally designed to adapt the micro-Mott spin detector to the HA-150 detector flange.

A particularly attractive feature of the micro-Mott design is that the high voltage (20 kV) is limited to a single internal electrode — the gold foil. Electrons are decelerated after scattering by the same electric field that accelerates them. The Sherman function and efficiency of the micro-Mott polarimeters have been studied extensively,[10,16] and by using this well-characterized design, we are able to use the accurately known parameters provided our polarimeter achieves the same beam characteristics at the Au foil as were obtained in the calibration exercises.

We have used electron trajectory simulation based on the ray-tracing program SIMION[17] to optimize lens col-

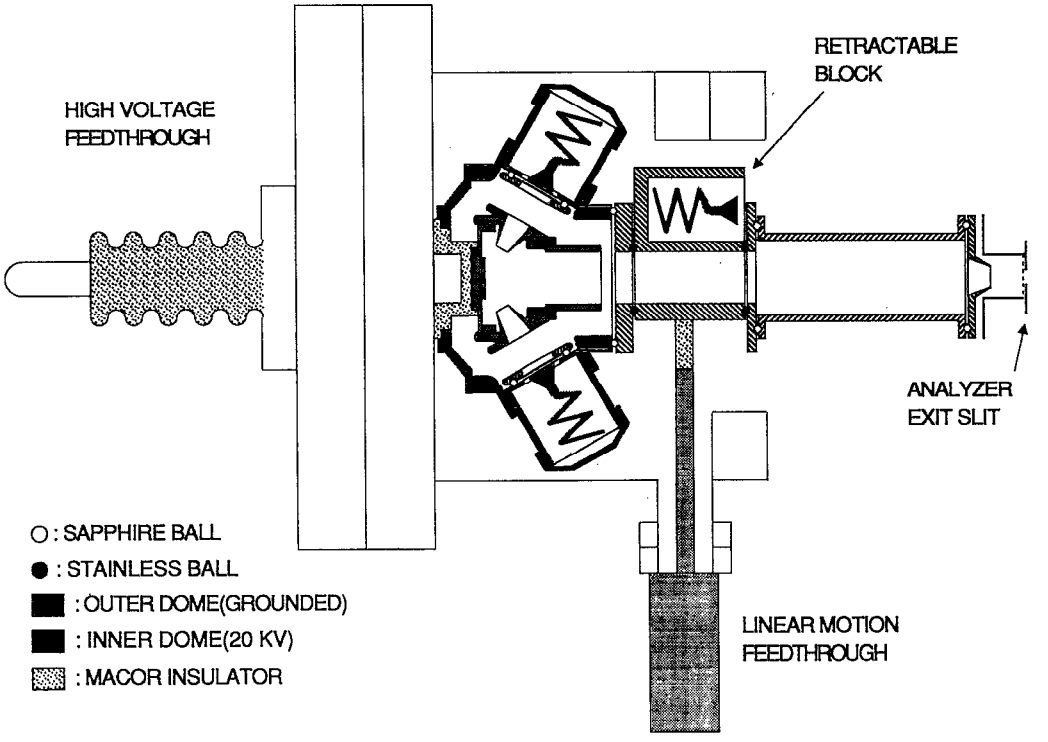

FIG. 2. Cross-sectional view of the modified micro-Mott polarimeter. The lens block is retractable along a direction perpendicular to the incident beam axis and functions both as the second lens element and as the channeltron housing. Only one opposing pair of channeltrons are shown in the cross-sectional view. All lens elements and apertures are electrically isolated by sapphire balls.

umn voltages in both conventional (spin-integrated) and spin-resolved detection modes. In conventional analyzer operation, the lens system must focus electrons from the exit slit into the channeltron at a suitable kinetic energy. In the spin detection mode, the lens column must provide a well-focused 20-kV beam at the Au target. Figures 3(a) and 3(b) illustrate representative ray-tracing analysis for the two operating modes, and Table I presents optimum input-lens voltages for both detection modes at selected analyzer pass energies. The trajectory analysis were carried out using assumed worst case source conditions, i.e., $w=6$ mm and $\alpha=10°$, a value 25% larger than the optimum angle of 8°. For the analyzer pass energies studied, the electron beam focus at the Au foil was characterized by a maximum diameter of 1.4 mm and maximum angle of incidence of 4°. The beam-focusing properties of the new lens system coupled to the analyzer exit slit are slightly better than those of the polarimeter which has been previously calibrated.[10] This suggests that the effective Sherman function of our modified polarimeter is essentially the same as that of the Rice University micro-Mott polarimeter.

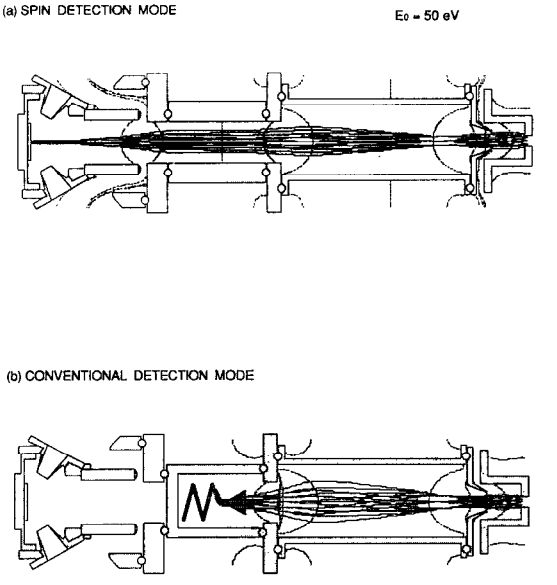

FIG. 3. Typical trajectories of the electrons emitted from the 6-mm-wide exit slit of the energy analyzer. The rays correspond to electrons emitted from five equally spaced points with emission at each point covering an angle of ±10°. The pass energy of the energy analyzer is 50 eV. (a) The transport and focal properties into the spin polarimeter. (b) The electron trajectories into the sliding channeltron. The voltages (with respect to the analyzer exit slit) on the entrance aperture, the first lens, and the second lens are 250, 850, and 3500 V, respectively, in (a); and 30, 0, and 500 V, respectively, in (b).

IV. PERFORMANCE

The analyzer/polarimeter performance has been tested in several experiments using both conventional detection and polarized electron detection. Conventional Auger electron spectroscopy and electron forward scattering[18] studies of surface structure have verified that analyzer performance is not altered by repositioning of the channeltron detector. Spin-polarized photoemission experiments and

TABLE I. The optimal input-lens voltages for spin-resolved and spin-integrated modes, and the corresponding spot diameter and incident angle for an electron beam focused on the scattering foil. All the voltages are with respect to the exit slit of the hemispherical analyzer.

Spin-resolved mode							
Pass energy (eV)	1	2	5	10	25	50	75
Entrance aperture (V)	5	10	10	25	250	250	300
First lens (V)	40	40	40	40	1000	850	1000
Second lens (V)	1310	1310	1310	1310	3500	3500	3500
Spot diameter (mm)	0.6	0.5	0.5	0.6	0.9	1.2	1.4
Incident Angle (deg)	0	1	1	3	2	4	4
Spin-integrated mode							
Entrance aperture	5	10	20	30	80	300	300
First lens (V)	20	20	20	20	20	0	0
Second lens (V)	500	500	500	500	500	500	750

spin-polarized secondary electron experiments have shown that the polarimeter accurately detects two orthogonal spin components.

The total path length from the target to the micro-Mott spin polarimeter is about 1 m. One concern in this design is therefore the possibility of spin precession due to stray magnetic fields along the path leading to inaccuracies in the detected spin. The magnetic shielding of the analyzer is adequate to reduce these effects to negligible values. The fact that residual polarization perpendicular to the easy axis of magnetization in a thin magnetic film is found to be essentially zero is a good indication of minimal spin precession in the analyzer.

V. FUTURE IMPROVEMENTS

The Rice-University-type retarding potential Mott polarimeters offer the advantages of large acceptance phase space, good discrimination against inelastically scattered electrons, insensitivity to surface conditions, near-ground-potential detection of scattered electrons, and a very stable Sherman function. However, its figure of merit is poor when compared to that of the LEED-type and low-energy diffuse scattering polarimeters. The figure of merit difference is attributable to a greater scattering efficiency in the low-energy polarimeters, which results from the large collection solid angle of the backscattered electrons. This suggests an avenue for improvement of ϵ achieved by the retarding potential Mott polarimeter.

The differential scattering cross section, $d\sigma/d\Omega$, and $S(\theta)$, where θ is the scattering angle, has been calculated for Au employing a Hartree–Fock potential. Figure 4 displays $d\sigma/d\Omega$ and $S(\theta)$ as a function of scattering angle θ for 20 keV electron scattering from a Au atom. These numerical results reveal that $S(\theta)$ and $d\sigma/d\Omega$ are relatively independent of the scattering angle around 120°. Figure 5, which displays the results obtained by integrating $S(\theta)$ based on single scattering,[19] shows little degradation of the effective Sherman function S_{eff} and a significant increase of polarimeter figure of merit. However, the effective Sherman function of a Mott detector is governed by multiple scattering. Therefore, the dependence of S_{eff} on polarimeter acceptance angle based on integrating S from a single-atom scattering over the detector acceptance may not accurately

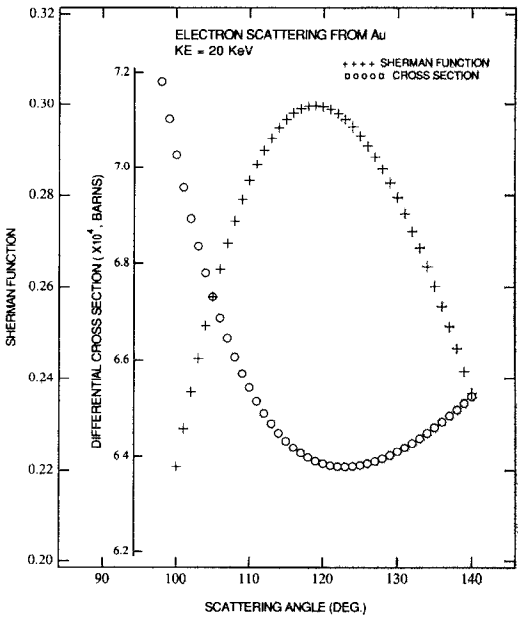

FIG. 4. The differential cross section $d\sigma/d\Omega$ and Sherman function $S(\theta)$ as a function of scattering angle for 20-keV electrons backscattered by Au (provided by A. W. Ross and M. Fink).

reflect the improvement in polarimeter figure of merit resulting from increasing the detected solid angle. In practice, we therefore expect that the small decrease in S_{eff} is more than compensated by the large increase in efficiency.

The ray-tracing results shown in Fig. 6(a) indicate that the effective acceptance angle of the current design is only 5° and *not* the 10° suggested by the geometry of the inner and outer apertures. Therefore, the collection efficiency of the current configuration is only 25% of the

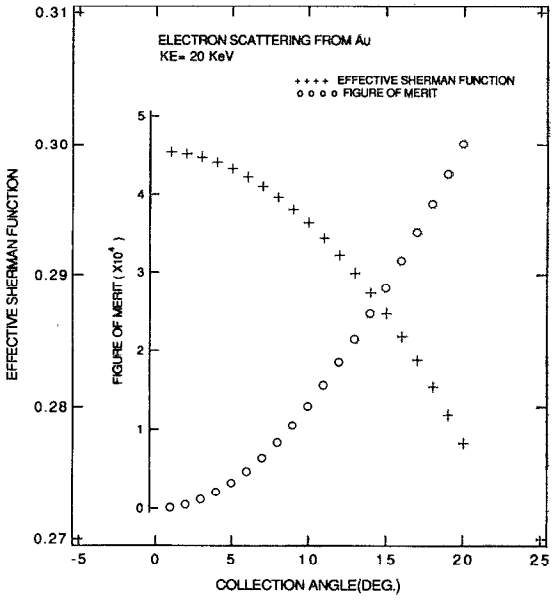

FIG. 5. The effective Sherman function S_{eff} and the figure of merit ϵ for different acceptance angles as defined in the text.

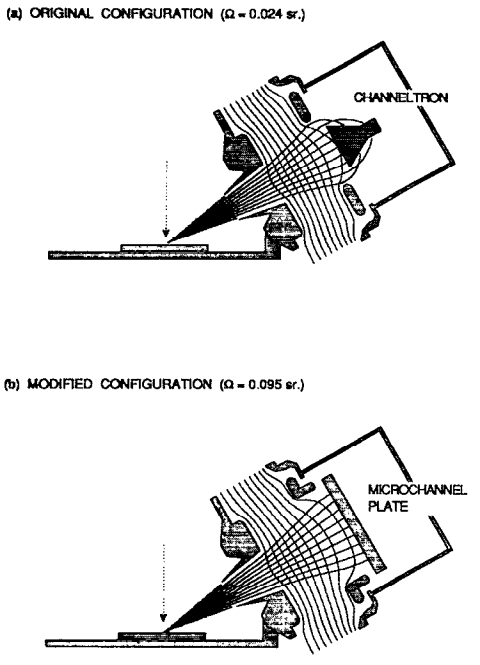

FIG. 6. The trajectories of electrons with 20 050-eV kinetic energy after scattering in the Mott polarimeter. The voltages on the inner and outer apertures are 20 and 1.3 kV, respectively. The channeltron in (a) and the microchannel plate in (b) are at the same potential as the outer aperture.

geometry-defined value. A significant improvement in polarimeter performance can be achieved if the scattered electrons are more efficiently collected. In practice, this could be accomplished by increasing the opening of the channeltron trumpet by a more efficient transport lens system to the channeltron or by replacing it with a microchannel plate. Space constraints of our present design limit the distance available for more efficient prechanneltron optics. Figure 6(b) displays ray-tracing results for replacement of the channeltron by a microchannel plate together with some minor modifications to the outer aperture geometry that increases the collection solid angle. After this minor change, the collection efficiency becomes nearly 100% of the geometry-limited value. This change should result in approximately a factor-of-4 improvement in the figure of merit. Even though these results are for a single scattering model, we expect enhancements in S_{eff} in a multiple-scattering environment (real foil) to be similar. This improvement would increase the efficiency of the micro-Mott polarimeter to a value equal to that of low-energy spin polarimeters.

ACKNOWLEDGMENTS

The authors are pleased to thank F. B. Dunning and G. K. Walters for providing the original drawings of their polarimeter and A. W. Ross and M. Fink for conducting the single scattering calculations. The work was supported by National Science Foundation Grant No. DMR93-03091.

[1] J. Kessler, *Polarized Electrons*, 2nd ed. (Springer, Berlin, 1985).
[2] *Polarized Electrons in Surface Physics*, edited by R. Feder (World Scientific, Singapore, 1985).
[3] N. F. Mott, Proc. R. Soc. London Ser. A **124**, 425 (1929); **135**, 429 (1932).
[4] M. R. Scheinfein, D. T. Pierce, J. Unguris, J. J. McClelland, R. J. Celotta, and M. H. Kelley, Rev. Sci. Instrum. **60**, 1 (1990).
[5] M. R. Scheinfein, J. Unguris, M. H. Kelley, D. T. Pierce, and R. J. Celotta, Rev. Sci. Instrum. **61**, 2501 (1990).
[6] J. Kirschner and R. Feder, Phys. Rev. Lett. **42**, 1008 (1979).
[7] J. Sawler and D. Venus, Rev. Sci. Instrum. **62**, 2409 (1991).
[8] E. Kisker, G. Baum, A. H. Mahan, W. Raith, and B. Reihl, Phys. Rev. B **18**, 2256 (1978).
[9] L. G. Gray, M. W. Hart, F. B. Dunning, and G. K. Walters, Rev. Sci. Instrum. **55**, 88 (1984).
[10] F.-C. Tang, X. Zhang, F. B. Dunning, and G. K. Walters, Rev. Sci. Instrum. **59**, 504 (1988); F. B. Dunning, L. G. Gray, J. M. Ratliff, F.-C. Tang, X. Zhang, and G. K. Walters, Rev. Sci. Instrum. **58**, 1706 (1987).
[11] J. Ungaris, D. T. Pierce, and R. J. Celotta, Rev. Sci. Instrum. **57**, 1314 (1986).
[12] T. J. Gay and F. B. Dunning, Rev. Sci. Instrum. **63**, 1635 (1992).
[13] D. W. O. Heddle, J. Phys. E **4**, 589 (1971).
[14] H. D. Polaschegg, Appl. Phys. **9**, 223 (1976).
[15] A. Gellrich, K. Jost, and J. Kessler, Rev. Sci. Instrum. **61**, 3399 (1990).
[16] D. M. Oro, W. H. Butler, F. B. Dunning, and G. K. Walters, Rev. Sci. Instrum. **62**, 667 (1991).
[17] SIMION is written by D. A. Dahl and J. E. Delmore, Idaho National Laboratory EG&G Idaho, Inc., P.O. Box 1625, Idaho Falls, ID 83415.
[18] W. F. Egelhoff, Jr., Crit. Rev. Solid State Mater. Sci. **14**, 269 (1988).
[19] D.-J. Huang, Ph.D. dissertation, University of Texas at Austin, 1994.